eV Hubble scale inflation with a radiative plateau: Very light inflaton, reheating, and dark matter in $B-L$ extensions

Anish Ghoshal,[1,*] Nobuchika Okada,[2,†] and Arnab Paul[3,‡]

[1]*Institute of Theoretical Physics, Faculty of Physics, University of Warsaw, ul. Pasteura 5, 02-093 Warsaw, Poland*

[2]*Department of Physics and Astronomy, University of Alabama, Tuscaloosa, Alabama 35487, USA*

[3]*Indian Statistical Institute, 203 B.T. Road, Kolkata-700108, India*

(Received 15 July 2022; accepted 18 October 2022; published 18 November 2022)

We study radiative plateaulike inflation and Z_{BL}-portal freeze-in fermionic dark matter in a minimal $B-L$ extended model. The $U(1)_{B-L}$ Higgs, responsible for heavy neutrino masses, also drives inflation in the early Universe, thanks to radiative corrections from the heavy neutrinos and the Z_{BL} gauge boson. In our benchmark choice for the $U(1)_{B-L}$ gauge coupling $g_{B-L} \sim 10^{-4}$, a light Z_{BL} boson can be explored by current and future lifetime frontier experiments, such as the Forward Search Experiment (FASER) and FASER 2 at the LHC, SHiP, Belle II, and LHCb. For the benchmark, the Hubble scale of inflation ($\mathcal{H}_{\rm inf}$) is very low [$\mathcal{H}_{\rm inf} = \mathcal{O}(100)$ eV] and the inflaton turns out to be very light with mass of $\mathcal{O}(1)$ eV, and consequently the decay width of the inflaton is extremely small. We investigate a two-field system with the inflaton/$B-L$ Higgs and the Standard Model (SM) Higgs, and find that the reheating with a sufficiently high temperature occurs when the waterfall direction to the SM Higgs direction opens up in the trajectory of the scalar field evolution.

DOI: 10.1103/PhysRevD.106.095021

I. INTRODUCTION

It has long been well known that the candidate responsible for the initial accelerated expansion of the Universe (inflation) may be associated with a scalar field (inflaton) [1,2]. Although the exact nature of this field remains a mystery, with the plethora of cosmological data available we are in a position to study and distinguish between the ultraviolet (UV) properties of various inflationary models. From particle theory point of view, it is often fancied that the inflaton field is also associated with solving other familiar issues in the Standard Model (SM). In this paper, we investigate a model where the SM neutrinos receive mass in a type-I seesaw framework, in a minimal gauged $(B-L)$ extension, and provide a Z_{BL}-portal freeze-in dark matter (DM) candidate. The bosonic and fermionic quantum corrections, respectively, from the Z_{BL} and the heavy neutrinos help to make the inflaton potential flat and inflation occurs in a radiative plateaulike region. This gives us the very interesting possibility of verifying inflationary predictions with laboratory searches in a UV-complete particle model. Moreover, this model contains a promising dark matter candidate, the so-called Z_{BL}-portal fermion DM.

Inflation scenarios driven by the quartic potential of the inflaton are highly disfavored by the cosmic microwave background (CMB) data as they predict too large tensor-to-scalar ratio [3].[1] The so-called inflection-point inflation is a diligent way to fit the CMB power spectrum by flattening the effective inflaton quartic potential with radiative corrections from bosonic and fermionic loops (among other ways) [13–32].[2] It was shown that, even with negligible nonminimal coupling values, the model can fit the CMB data.[3]

Using bosonic and fermionic corrections to achieve the inflection point was studied in Refs. [16,17,24]; particularly, $B-L$ gauged U(1) Higgs inflation has been studied in this setup, giving the predictions consistent with the

*anish.ghoshal@fuw.edu.pl

†okadan@ua.edu

‡arnabpaul9292@gmail.com

[1]By introducing a coupling of the inflaton field to the Ricci scalar (nonminimal gravitational coupling), tensor-to-scalar ratio r values can be lowered [1,4–12].

[2]See Refs. [33,34] for inflation in Grand Unified Theory framework with DM.

[3]Of course, a nonminimal gravitational coupling should be nevertheless be present in a complete analysis, since it is radiatively generated, even if it is set to zero at some scale. Nevertheless, such a coupling is only important in the trans-Planckian regime.

CMB observations [28,35,36], as well as a collider search for a long-lived inflaton [37]. As we will see, inflation demands a tiny gauge coupling, which in turn dictates us to embed the inflationary setup in a small field inflation scenario, resulting a small inflaton mass and incurring the following:

(i) If the reheating proceeds via the inflaton decay, the inflaton is too light to have produced the visible Universe.
(ii) The tiny gauge coupling makes it hard for the Z_{BL}-portal DM particle to get in the thermal plasma of the SM particles.

In this article, we study the inflection-point inflation and how to resolve the aforementioned issues by closely scrutinizing the early Universe dynamics. We will show that, even if the inflaton is extremely light, it is possible to have a reheating temperature to be sufficiently high due to opening up of the waterfall direction in the SM Higgs direction in the scalar field trajectory of oscillation after inflation.

For the parameter choice in this work, we find that for a typical DM mass of $m_\chi = \mathcal{O}(10)$ GeV, Z_{BL} is thermalized in the SM plasma at $T \sim m_\chi$. By setting a suitable $B-L$ charge for DM, DM (χ) can be produced with the right abundance via the freeze-in mechanism. We discuss a falsifiability of the model in future experiments. Because of the smallness of the coupling strengths, it is very challenging to see any direct laboratory signatures of such a freeze-in DM. However, one of the plausible pathways to detect the freeze-in DM is to have the DM production in the early Universe via the decays of dark sector particles that are in thermal equilibrium with the SM plasma. Such feeble couplings associated with the decays make the dark sector particles very long-lived and can be looked for at the Large Hadron Collider (LHC) and beyond (see [38–40]). On the other hand, if the freeze-in DM is produced via scattering processes with a dark sector particle as a mediator, then depending on the nature of the portal (scalar portal, vector portal, etc.) one can search for the mediator particles at the lifetime frontier and intensity frontier experiments [41–52].[4]

The paper is arranged as follows: in the next section, we describe a simple $B-L$ gauged extension of the SM and describe how a plateau region can be created in the $B-L$ Higgs potential due to quantum corrections from the heavy neutrinos and the $B-L$ gauge boson. In the following section, we investigate the scalar field trajectory after inflation to see how a successful reheating can occur in a "two-field" system with the $B-L$ and SM Higgs fields. Next, we discuss the formation of DM via the freeze-in mechanism and experimental searches in the model parameter space and end our study with conclusions in the final section.

[4]See Ref. [53] for other tests of freeze-in DM.

II. CREATING POINT OF INFLECTION IN GAUGED HIGGS POTENTIAL

In order to realize the inflection point in a Higgs potential, we employ the renormalization-group (RG)-improved effective Higgs potential. For a quartic potential, the quartic coupling first decreases (due to fermionic corrections) and then increases in the UV (due to bosonic corrections). It is well known that, in the vicinity of the minimum point of the running quartic coupling, both the quartic coupling and its beta function become vanishingly small, due to which an inflection point can be realized in the effective Higgs potential. It is at this point that the relation between high and low energy physics become manifest: the quantum corrections in a particle model determine the point of inflection and the scale of inflation.

A. The model

Minimal $B-L$ extension of the SM provides the ingredients for neutrino masses and lepton number violation [54–59]. Following [43], we add a dark Dirac fermion χ [SM singlet, but charged under $U(1)_{B-L}$] as our DM candidate via the $B-L$ gauge interaction (Z_{BL} portal).

The right-handed neutrinos (N_R^i) have Majorana Yukawa interaction terms,

$$\mathcal{L} \supset -\frac{1}{2}\sum_{i=1}^{3} Y_i \varphi \overline{N_R^{iC}} N_R^i + \text{H.c.} \tag{1}$$

Associated with the gauge symmetry breaking, all the new particles, $B-L$ gauge boson (Z_{BL}), the right-handed neutrinos (N_R), and the $B-L$ Higgs acquire their masses, which are as follows:

$$m_{Z_{BL}} = 2 g_{BL} v_{BL}, \quad m_{N^i} = \frac{1}{\sqrt{2}} Y_i v_{BL}, \quad m_\phi = \sqrt{2\lambda_\phi} v_{BL}, \tag{2}$$

where λ_ϕ is the quartic coupling of the $B-L$ Higgs field φ (see the next section), and $v_{BL} = \sqrt{2}\langle\varphi\rangle$ is the vacuum

TABLE I. Particle content of the model. $i = 1, 2, 3$ is the generation index.

	$SU(3)_c$	$SU(2)_L$	$U(1)_Y$	$U(1)_{B-L}$
q_L^i	3	2	$+1/6$	$+1/3$
u_R^i	3	1	$+2/3$	$+1/3$
d_R^i	3	1	$-1/3$	$+1/3$
ℓ_L^i	1	2	$-1/2$	-1
N_R^i	1	1	0	-1
e_R^i	1	1	-1	-1
H	1	2	$-1/2$	0
φ	1	1	0	$+2$
χ	1	1	0	Q_χ

expectation value (VEV) of the $B-L$ Higgs field. The $B-L$ Higgs field φ can be redefined as $\varphi=(\phi+v_{BL})/\sqrt{2}$ in the unitary gauge, and we identify the real scalar field ϕ to be the inflaton.

When the SM is extended with the gauged $U(1)_{B-L}$ symmetry, there is no anomaly associated with the $B-L$ gauge symmetry due to the presence of three SM-singlet right-handed neutrinos with $B-L$ charges of -1. On top of this, as mentioned before, we introduce a SM-singlet Dirac fermion χ: our DM candidate. The interaction part of the Lagrangian includes

$$\mathcal{L}_{Z_{BL}} = y_l \bar{L}\tilde{H}N + g_{BL}(Z_{BL})_\mu \times\left[\sum_f (B-L)_f \bar{f}\gamma^\mu f + Q_\chi \bar{\chi}\gamma^\mu\chi\right] + \text{H.c.}, \quad (3)$$

where g_{BL}, Q_χ, $m_{Z_{BL}}$, and m_χ are the free parameters of the model. The particle content of the model is shown in Table I.

B. Slow-roll parameters and constraints from Planck 2018

The inflationary slow-roll parameters are given by

$$\epsilon(\phi)=\frac{M_P^2}{2}\left(\frac{V'}{V}\right)^2,\quad \eta(\phi)=M_P^2\left(\frac{V''}{V}\right),\quad \varsigma^2(\phi)=M_P^4\frac{V'V'''}{V^2}, \quad (4)$$

where $M_P=M_{\rm Pl}/\sqrt{8\pi}=2.43\times10^{18}$ GeV is the reduced Planck mass, V is the inflation potential, and the prime is the derivative with respect to inflaton ϕ.

The curvature perturbation $\Delta^2_{\mathcal{R}}$ is given by

$$\Delta^2_{\mathcal{R}}=\frac{1}{24\pi^2}\frac{1}{M_P^4}\frac{V}{\epsilon}\bigg|_{k_0}, \quad (5)$$

which must satisfy $\Delta^2_{\mathcal{R}}=2.189\times10^{-9}$ from the Planck 2018 results [3] at pivot scale $k_0=0.05\ \text{Mpc}^{-1}$. The number of e-folds is given by

$$N=\frac{1}{M_P^2}\int_{\phi_E}^{\phi_I}\frac{V}{V'}d\phi, \quad (6)$$

where ϕ_I is the value of the inflaton during the horizon exit of the scale k_0, and ϕ_E is defined as the value of the inflaton when the slow-roll condition is violated, i.e., $\epsilon(\phi_E)=1$.

The slow-roll approximation holds when $\epsilon\ll1$, $|\eta|\ll1$, and $\varsigma^2\ll1$. The inflationary predictions are given by

$$n_s=1-6\epsilon+2\eta,\qquad r=16\epsilon,\qquad \alpha=16\epsilon\eta-24\epsilon^2-2\varsigma^2, \quad (7)$$

where n_s and r and $\alpha\equiv\frac{dn_s}{dlnk}$ are the scalar spectral index, the tensor-to-scalar ratio, and the running of the spectral index, respectively, at $\phi=\phi_I$. The Planck 2018 results [3] give an upper bound on $r\lesssim0.067$; the bounds for the spectral index (n_s) and the running of the spectral index (α) are 0.9691 ± 0.0041 and 0.0023 ± 0.0063, respectively. A joint study with the dataset of Planck, BICEP/Keck 2018, and baryon acoustic oscillations pulls down the upper bound of the tensor-to-scalar ratio to $r<0.032$ [60]. Future precision measurements have the potential to pin down the error in α to ±0.002 [61,62].

C. Achieving the plateau

The scalar potential for inflection-point inflation at an inflection point near $\phi=M$ is given by [28]

$$V(\phi)\simeq V_0+\sum_{n=1}^{3}\frac{1}{n!}V_n(\phi-M)^n, \quad (8)$$

where $V_0=V(M)$ is a constant, $V_n\equiv d^nV/d\phi^n|_{\phi=M}$ are derivatives evaluated at $\phi=M$, and $\phi=M$ is the inflaton field value at the pivot scale $k_0=0.05\ \text{Mpc}^{-1}$ of the Planck 2018 measurements [3]. If the values of V_1 and V_2 are tiny enough, the (almost) inflection point can be realized. Rewriting Eqs. (4) and (8), we get

$$\epsilon(M)\simeq\frac{M_P^2}{2}\left(\frac{V_1}{V_0}\right)^2,\qquad \eta(M)\simeq M_P^2\left(\frac{V_2}{V_0}\right),$$
$$\chi^2(M)=M_P^4\frac{V_1V_3}{V_0^2}, \quad (9)$$

where we have used the approximation $V(M)\simeq V_0$. Similarly, the power spectrum $\Delta^2_{\mathcal{R}}$ is expressed as

$$\Delta^2_{\mathcal{R}}\simeq\frac{1}{12\pi^2}\frac{1}{M_P^6}\frac{V_0^3}{V_1^2}. \quad (10)$$

Using the observational constraint $\Delta^2_{\mathcal{R}}=2.189\times10^{-9}$ and a fixed n_s value, we obtain

$$\frac{V_1}{M^3}\simeq1963\left(\frac{M}{M_P}\right)^3\left(\frac{V_0}{M^4}\right)^{3/2},$$
$$\frac{V_2}{M^2}\simeq-1.545\times10^{-2}\left(\frac{1-n_s}{1-0.9691}\right)\left(\frac{M}{M_P}\right)^2\left(\frac{V_0}{M^4}\right), \quad (11)$$

where we have used $V(M)\simeq V_0$ and $\epsilon(M)\ll\eta(M)$. For the remainder of the analysis, we set $n_s=0.9691$, the central value from the Planck 2018 results [3]. We neglect the $O(10\%)$ level uncertainty in the values of cosmological inflationary parameters in this analysis, as it will not change the highlight of this work. Then V_3 becomes

$$\frac{V_3}{M} \simeq 6.983 \times 10^{-7} \left(\frac{60}{N}\right)^2 \left(\frac{V_0^{1/2}}{M M_P}\right). \tag{12}$$

Using Eqs. (7), (9), (11), and (12), the tensor-to-scalar ratio (r) is given by

$$r = 3.082 \times 10^7 \left(\frac{V_0}{M_P^4}\right), \tag{13}$$

and the running of the spectral index (α) is

$$\alpha \simeq -2\varsigma^2(M) = -2.741 \times 10^{-3} \left(\frac{60}{N}\right)^2. \tag{14}$$

Note that the running is independent of V_0 and M. This prediction is consistent with the current experimental bound, $\alpha = 0.0023 \pm 0.0063$ [3]. Precision measurements of the running of the spectral index in future experiments can reduce the error to ± 0.002 [61,62]. Hence, the prediction can be tested in the future.

D. Radiative plateau

For creating the plateau in the $\mathrm{U}(1)_{B-L}$ Higgs potential $V_{\mathrm{tree}} = \frac{1}{4}\lambda_{\phi-\mathrm{tree}}\phi^4$, let us take a look at the renormalization-group equation (RGE)-improved effective potential,

$$V(\phi) = \frac{1}{4}\lambda_\phi(\phi)\phi^4, \tag{15}$$

where $\lambda_\phi(\phi)$ is the solution to the RGEs, which involves the beta functions of g_{BL}, Y, and λ_ϕ, $\beta_{g_{BL}}$, β_Y, and β_{λ_ϕ}, respectively. For simplicity, we assume the degenerate mass spectrum for the right-handed neutrinos, $Y \equiv Y_1 = Y_2 = Y_3$. The coefficients in the expansion of Eq. (8) are given as[5]

$$\begin{aligned}
\frac{V_1}{M^3} &= \frac{1}{4}(4\lambda_\phi + \beta_{\lambda_\phi}),\\
\frac{V_2}{M^2} &= \frac{1}{4}(12\lambda_\phi + 7\beta_{\lambda_\phi} + M\beta'_{\lambda_\phi}),\\
\frac{V_3}{M} &= \frac{1}{4}(24\lambda_\phi + 26\beta_{\lambda_\phi} + 10M\beta'_{\lambda_\phi} + M^2\beta''_{\lambda_\phi}),
\end{aligned} \tag{16}$$

where the prime denotes the differential coefficient $d/d\phi$. Using $V_1/M^3 \simeq 0$ and $V_2/M^2 \simeq 0$, we obtain

$$\beta_{\lambda_\phi}(M) \simeq -4\lambda_\phi(M), \qquad M\beta'_{\lambda_\phi}(M) \simeq 16\lambda_\phi(M). \tag{17}$$

Hence, the last equation in Eq. (16) is simplified to $V_3/M \simeq 16\lambda_\phi(M)$. Comparing it with Eq. (12), we obtain

[5]For details of this derivation, see Ref. [28].

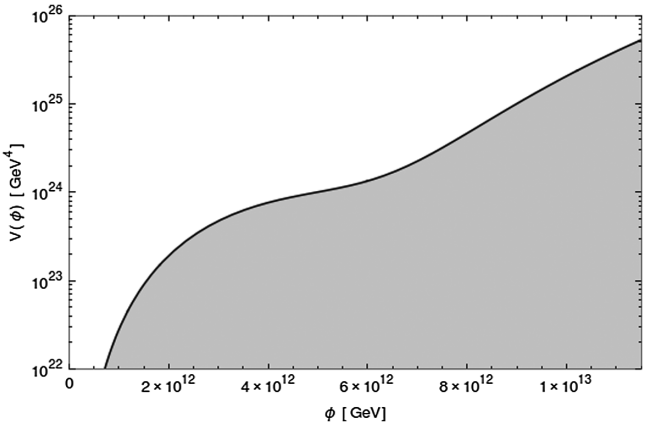

FIG. 1. RG-improved $B-L$ inflaton potential as a function of ϕ. Here, we have fixed $M = 2.78 \times 10^{-6} M_P$, so that $g_{BL} = 10^{-4}$, $Y = 2.3 \times 10^{-4}$, and $\lambda_\phi(M) = 3.7 \times 10^{-27}$. We note that the inflection-point-like point appears at $\phi \sim M$.

$$\lambda_\phi(M) \simeq 4.762 \times 10^{-16} \left(\frac{M}{M_P}\right)^2 \left(\frac{60}{N}\right)^4, \tag{18}$$

where we have approximated $V_0 \simeq (1/4)\lambda_\phi(M)M^4$. Since the $\lambda_\phi(M)$ is extremely small, we approximate $\beta_{\lambda_\phi}(M) \simeq 0$, which leads to

$$Y(M) \simeq 32^{1/4} g_{BL}(M). \tag{19}$$

For this relation between g_{BL} and Y, we have assumed that the gauge and the Yukawa couplings dominate the beta function; as a consequence, the mass ratio of the right-handed neutrinos and the $B-L$ gauge boson is fixed in order to have a plateau inflation.

Using the second equation in Eqs. (17) and (19), we find $\lambda_\phi(M) \simeq 3.713 \times 10^{-3} g_{BL}(M)^6$. Then from Eq. (18), $g_{BL}(M)$ is expressed as

$$g_{BL}(M) \simeq 7.107 \times 10^{-3} \left(\frac{M}{M_P}\right)^{1/3}. \tag{20}$$

Finally, from Eqs. (13) and (18), the tensor-to-scalar ratio (r) is given by

$$r \simeq 3.670 \times 10^{-9} \left(\frac{M}{M_P}\right)^6, \tag{21}$$

which is very small, as expected in the single-field inflationary scenarios. For a sample parameter choice, we plot the effective potential in Fig. 1.

III. REHEATING DYNAMICS OF THE SCALAR FIELDS

In order to investigate the reheating dynamics, we start with the two-dimensional field space with the scalar potential of the model given by

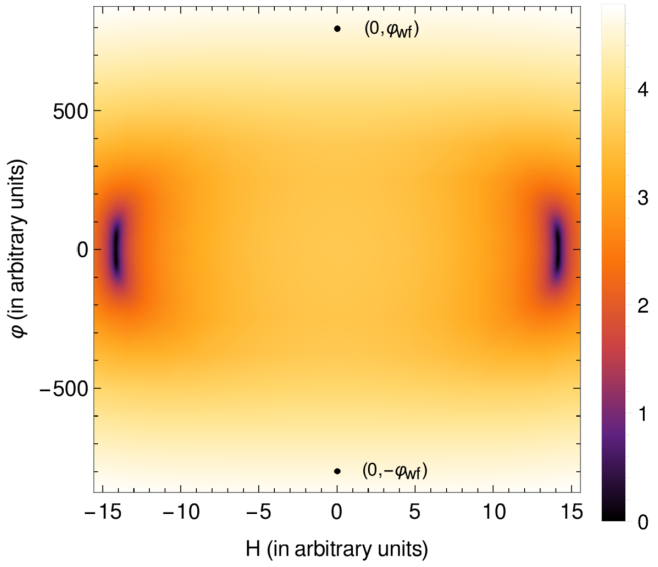

FIG. 2. Plot of $\log_{10}(V+1)$ as function of H and φ (toy model) in color coding.

$$V(|H|,|\varphi|) = \lambda_\phi\left(|\varphi|^2 - \frac{v_{BL}^2}{2}\right)^2 + \lambda_H\left(|H|^2 - \frac{v_H^2}{2}\right)^2 + \sqrt{4\lambda_H\lambda_\phi\xi}\left(|H|^2 - \frac{v_H^2}{2}\right)\left(|\varphi|^2 - \frac{v_{BL}^2}{2}\right), \tag{22}$$

where H is the SM Higgs, φ is the inflaton [$U(1)_{B-L}$ gauged Higgs], v_H and v_{BL} are their VEVs, respectively, λ_ϕ and λ_H are their respective quartic couplings, and $\sqrt{4\lambda_H\lambda_\phi\xi}$ is the quartic mixing of φ and H. After inflation, the field rolls down along the inflaton direction toward $\varphi = 0$. We numerically solve the equations of the motion of this two-field system with the SM Higgs boson decay width Γ_H, but neglect the inflaton decay width. The equations are given by

$$\ddot{\varphi} + 3\mathcal{H}\dot{\varphi} + V_{,\varphi} = 0, \tag{23}$$

$$\ddot{H} + (3\mathcal{H} + \Gamma_H)\dot{H} + V_{,H} = 0. \tag{24}$$

Although there is a "bump" (local maximum) around (0,0) in the potential as shown in Fig. 2, at the initial stage, due to high inertia in the φ direction, the oscillation occurs mostly along the φ direction. With time, this oscillation amplitude along φ dies down slowly due to Hubble friction until the φ amplitude becomes similar to the order of the length of the potential bump along the φ axis. At this stage, the field feels the slope of the potential around the potential bump. During this oscillation, before the field reaches the $\varphi = 0$ value, the waterfall direction opens up in the SM Higgs direction, which is at

$$\varphi = \varphi_{wf} \equiv \frac{1}{\sqrt{2}}\sqrt{v_{BL}^2 + \frac{\lambda_H v_H^2}{\sqrt{\lambda_H\lambda_\phi\xi}}}. \tag{25}$$

If the field is displaced by a tiny amount from the inflaton (φ) axis (due to fluctuations), the field rolls down in the waterfall direction (with additional rapid oscillation parallel to the SM Higgs direction) and the field follows an approximately semielliptic path (this path is truly semi-elliptic for $\xi = 1$) of semimajor axis $2\times\varphi_{wf}$ and semi-minor axis $2\times H_{\rm minor}$, where

$$H_{\rm minor} \equiv \frac{\sqrt{v_{BL}^2\sqrt{\lambda_H\lambda_\phi\xi} + \lambda_H v_H^2}}{\sqrt{2\lambda_H}}, \tag{26}$$

around the (0,0) point of the field space to reach $\varphi = -\varphi_{wf}$. The additional oscillation in the SM Higgs direction about the smooth semielliptical path dies down quickly due to the decay rate of the SM Higgs Γ_H, after which only the smooth elliptical path dynamics is left. The trajectory of the field from the numerical solutions is shown in Fig. 3 with a set of arbitrary values of parameters (termed "toy model" in Figs. 3 and 4). The toy model is chosen in such a way that the total timescale ($\Delta t_{\rm sol}$) we solved Eqs. (23) for satisfies $\mathcal{H}_{wf}^{-1} \gg \Delta t_{\rm sol} \sim \tilde{\Gamma}_{\rm eff}^{-1}$, where $\mathcal{H}_{wf}$ and $\tilde{\Gamma}_{\rm eff}$ are defined in Eqs. (28) and (27), respectively. This choice

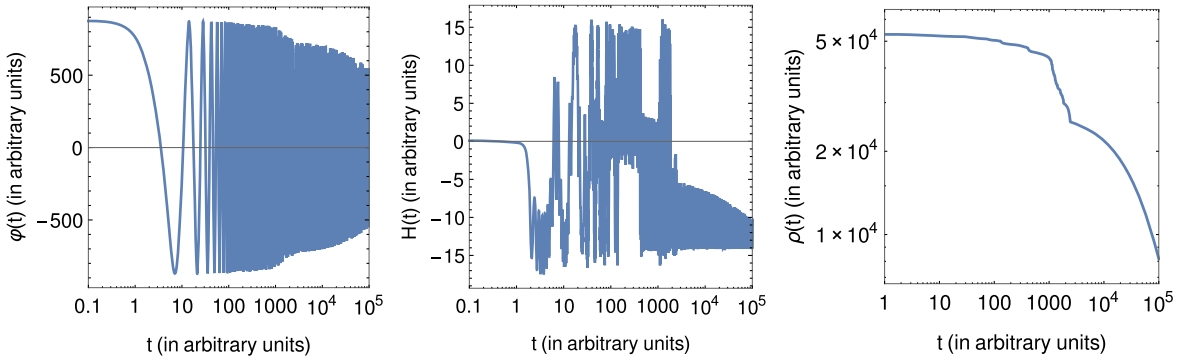

FIG. 3. Evolution of the two fields $\varphi(t)$ and $H(t)$ and the energy density $\rho(t)$ with time t for a toy model.

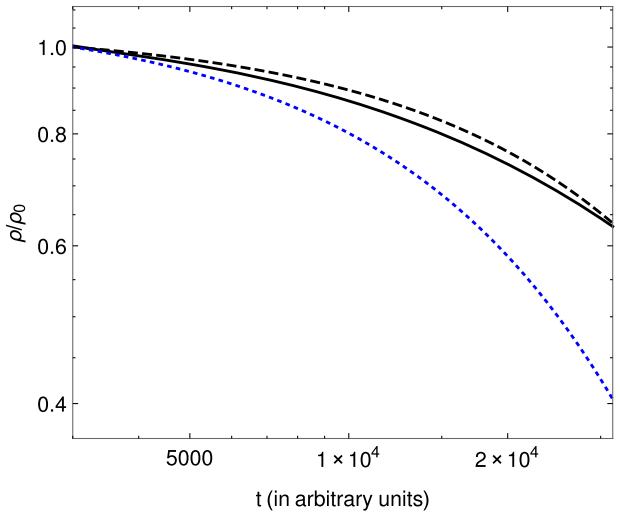

FIG. 4. Black solid curve denotes the numerical solution of ρ vs t for the toy model (with a normalization factor ρ_0). The blue dotted curve is $e^{-\tilde{\Gamma}_{\rm eff}t}$, whereas the black dashed curve is $e^{-0.5\tilde{\Gamma}_{\rm eff}t}$. It is clear from these plots that the approximate formula of $\Gamma_{\rm eff}$ given by Eq. (27) describes the decay within a factor of 2.

enables us to observe the effect of energy dilution in the fields resulting directly from the decay, not due to Hubble friction. This choice ($\mathcal{H}_{wf}^{-1} > \tilde{\Gamma}_{\rm eff}^{-1}$) is also satisfied in the realistic case we discuss later on. Although the values of the parameters used for the plots in this subsection are arbitrary (toy model), the physical characteristics of the dynamics are similar for our realistic choice of the parameters.

As the tangent vector of this approximate semielliptic path in the two-field system has a component in the SM Higgs direction, even if the decay rate of inflaton $\Gamma_\phi = 0$,[6] the oscillation along the elliptical path dies down quickly due to the "effective decay rate" arising from the friction in the SM Higgs direction,

$$\Gamma_{\rm eff} \sim \Gamma_H \left(\frac{H_{\rm minor}}{\varphi_{wf}}\right)^2 \equiv \tilde{\Gamma}_{\rm eff}. \tag{27}$$

This quick depletion of energy density starting from near $t = 2000$ (in arbitrary units), as shown in Fig. 3, can be interpreted as the reheating of the Universe.

We see in Fig. 4 that this approximate formula of $\Gamma_{\rm eff}$ mimics the numerically estimated energy depletion within a factor of $\mathcal{O}(1)$. If the Hubble parameter at the waterfall $\mathcal{H}_{wf} \ll \Gamma_{\rm eff}$, i.e., decay timescale is negligible with respect to the Hubble timescale, we can assume instantaneous reheating. We then estimate the reheating temperature as

$$T_{rh} = 0.55\left(\frac{100}{g_*}\right)^{1/4}\sqrt{\mathcal{H}_{wf}M_P} \times \left[\text{when } \Gamma_{\rm eff} \gg \mathcal{H}_{wf} \equiv \frac{1}{\sqrt{3}M_P}\sqrt{V(0,\varphi_{wf})}\right]. \tag{28}$$

We emphasize that the nontrivial field dynamics, and hence the effective decay rate $\Gamma_{\rm eff}$, enables the reheating temperature to be greater than the big bang nucleosynthesis (BBN) energy scale, even if the actual decay rate of the inflaton itself is unable to do so. Below we give a benchmark point for our study.

A. Case study for benchmark point

For our benchmark point $g_{BL} = 10^{-4}$, $Y = 2.3 \times 10^{-4}$, and $\lambda_\phi = 3.7 \times 10^{-27}$ during inflation, at lower energy[7] for $\lambda_\phi = 1.8 \times 10^{-23}$, $v_{BL} = 10^3$ GeV, $\lambda_H = 0.1$, $v_H = 246$ GeV, and $\xi = 0.1$, we get $\Gamma_{\rm eff} = 1.72 \times 10^{-14}$ GeV. We note that, for our choice of the benchmark point, the mass of the inflaton is $m_\phi = \sqrt{2\lambda_\phi}v_{BL} \sim 6 \times 10^{-9}$ GeV and inflation happens at the Hubble parameter $\mathcal{H}_{\rm inf} \sim 7 \times 10^{-7}$ GeV (scale of inflation). For this value of m_ϕ, the inflaton may decay only into photons or neutrinos (via mixing with the SM Higgs). The mixing angle between the inflaton and SM Higgs is also negligible at this value: $\theta \sim \sqrt{\xi}\frac{m_\phi}{m_H} \sim 1.5 \times 10^{-11}$. Hence, the inflaton decay rate is very suppressed and, as a result, reheating of the Universe from straightforward decay of the inflaton is difficult, and so is its compatibility with the BBN constraints.

However, as we showed via numerical estimates in the toy model in Sec. III, when the waterfall direction opens up, the Hubble parameter becomes $\mathcal{H}_{wf} = 6.9 \times 10^{-15}$ GeV, which is smaller than $\Gamma_{\rm eff}$. This means that, during this period, within one Hubble time, the energy density stored in the fields dilutes away, and the reheating temperature is approximated to be $T_{rh} = 0.55(\frac{100}{g_*})^{1/4}\sqrt{\mathcal{H}_{wf}M_P} \sim 70$ GeV, using Eq. (28).

IV. WEAKLY COUPLED $B-L$ PORTAL DARK MATTER

Because of the choice of the tiny gauge coupling g_{BL}, the DM particle has never been in thermal equilibrium. Hence, we consider the freeze-in mechanism for producing the DM particle via the Z_{BL} portal. We will provide a benchmark point that satisfies all the inflationary, reheating, and DM relic density constraints and will also discuss a possibility to hunt for the Z_{BL} gauge boson in future experimental facilities.

The dark matter physics in our scenario is very similar to the case considered in Ref. [43], and thus we follow the freeze-in DM scenario along with the conditions that the

[6]Note that the mass of the inflaton $m_\phi = \sqrt{2\lambda_\phi}v_{BL}$ is very small for small values of λ_ϕ, possibly making it kinematically inaccessible for the inflaton to decay in most channels through mixing with the SM Higgs (with mixing angle $\theta \sim \sqrt{\xi}\frac{m_\phi}{m_H}$).

[7]Evolving via the RGE.

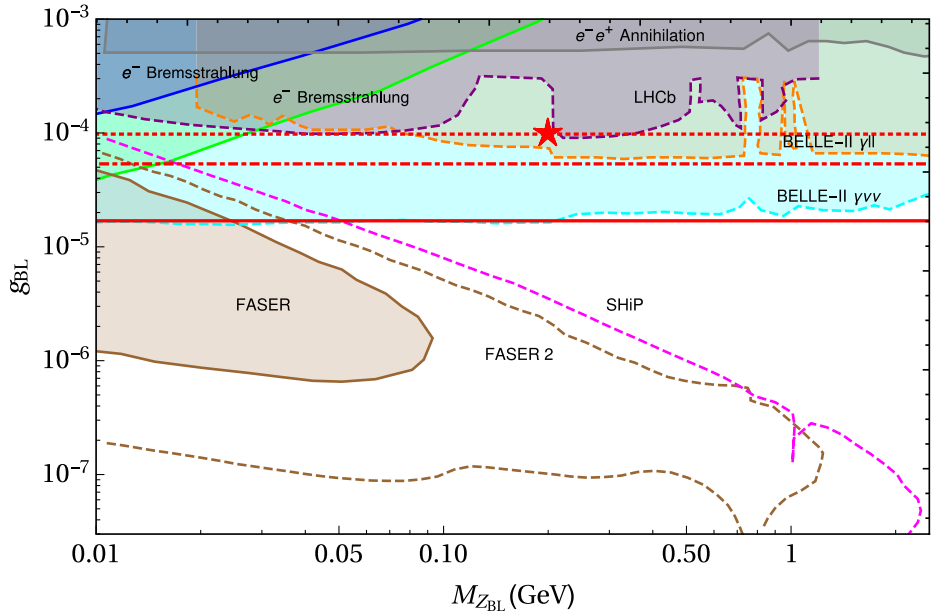

FIG. 5. Plot of parameter space of Z_{BL} searches. The three horizontal red lines from bottommost to topmost represent $\Omega_{\rm DM}h^2 = 0.12$ contours, where Q_χ values are, respectively, 10^{-2} (solid), 10^{-3} (dot-dashed), and 3×10^{-4} (dotted). Electron bremsstrahlung and annihilation results are obtained from DarkCast [63,64]. We show the sensitivity reaches of the several experiments in different color lines: FASER and FASER 2 [65] in solid and dashed brown lines; ShiP [66] in magenta dashed line; light blue and orange dashed lines for Belle II [67]; purple dashed line for LHCb [68,69]. The point marked with the red ⋆ represents the benchmark point we chose, as an example, where inflationary, reheating, and DM relic density constraints are satisfied.

Z_{BL} was in thermal equilibrium with SM particles with $g_{BL} \geq 2.7 \times 10^{-8}\sqrt{m_\chi[\mathrm{GeV}]}$ (see Ref. [43] for details). We assume zero initial abundance of DM at the time of reheating after inflation. There are two processes responsible for the DM production, $f\bar{f} \to \chi\bar{\chi}$ mediated by Z_{BL} and $Z_{BL}Z_{BL} \to \chi\bar{\chi}$, where f denotes SM fermions, and the corresponding cross sections are given by

$$\sigma(\bar{\chi}\chi \to f\bar{f})v \simeq \frac{37}{36\pi s}(Q_\chi g_{BL})^2 g_{BL}^2,$$
$$\sigma(\bar{\chi}\chi \to Z_{BL}Z_{BL})v \simeq \frac{(Q_\chi g_{BL})^4}{4\pi s}\left(\ln\left[\frac{s}{m_\chi^2}\right] - 1\right), \quad (29)$$

assuming $m_b^2 \ll m_\chi^2 < m_t^2$ and $m_{Z_{BL}}^2 \ll m_\chi^2$, m_b and m_t being the masses of the bottom and the top quarks, respectively. Here, we have used the approximation formulas in Eq. (29) as was shown in Ref. [43] to produce almost the same results as numerical computations.

Using these scattering processes, the DM relic ($\Omega_{\rm CDM}h^2 = 0.12$) constraint can be translated to the following relations (for details, see Ref. [43]):

$$(Q_\chi g_{BL})^2 g_{BL}^2 + \frac{0.82}{1.2}(Q_\chi g_{BL})^4 \simeq 8.2 \times 10^{-24}, \quad (30)$$

which is insensitive to the Z_{BL} boson mass. One can satisfy the DM relic density constraint by suitably choosing Q_χ (see Fig. 5). For our choice of $g_{BL} = 10^{-4}$, Eq. (30) is satisfied with $Q_\chi = 3 \times 10^{-4}$.

V. EXPERIMENTAL PROBES

In order to understand a possible pathway to probe our scenario, we consider the various laboratory-based experiments, which are the so-called lifetime frontier experiments, to search for long-lived particles (the Z_{BL} gauge boson in our model). These searches are based on the possibility that a new particle produced at the colliders travels and decays, exhibiting displaced vertex and/or missing energy signatures. We presented in Fig. 5 the current experimental constraints and future sensitivity reaches in the $(M_{Z_{BL}}, g_{BL})$ plane. Here, the experiments we consider are the Forward Search Experiment (FASER) and FASER 2 [65], SHiP [66], Belle II, and LHCb [67–69]. The planned FASER detector[8] and SHiP [65,66] at the LHC will be able to probe the low $M_{Z_{BL}}$ and low g_{BL} values. In Fig. 5, the horizontal red lines (solid, dot-dashed, and dotted) correspond to the results for the various Q_χ values of the DM particle χ, satisfying $\Omega_{\rm CDM}h^2 = 0.12$. For higher g_{BL} and low $M_{Z_{BL}}$ values, the electron bremsstrahlung modes provide tighter constraints, whereas for higher g_{BL} and $M_{Z_{BL}}$

[8]The FASER detector is in a tunnel near the ATLAS detector of the LHC and about 480 m away to look for displaced vertices with charged particles arising from long-lived neutral particles produced at the primary vertex of the LHC.

values, the electron-positron annihilation mode is more stringent (for details, see Refs. [63,64]). Our benchmark point, denoted by a red ⋆ in Fig. 5, will be within the reach of BELLE-II searches.

VI. DISCUSSIONS AND CONCLUSIONS

We investigated a minimal $B-L$ extension of the SM model and predicted the parameter space where the problems of dark matter, neutrino masses, inflation, and reheating can be accounted for. We summarize our findings in the following points below:

(i) A very low scale inflation can be driven by the effective flat potential of the $B-L$ Higgs field ϕ (which breaks due to bosonic and fermionic quantum corrections, in which the inflaton is extremely light: $m_\phi \sim 6\times 10^{-9}$ GeV for our benchmark point). This raises an issue that the reheating temperature from the inflaton decay is too low to satisfy the model-independent lower bound on $T_{re} \geq 1$ from the successful big bang nucleosynthesis. We showed that in a two-field system, due to the elliptic shape of the valley near the minima, the field oscillates also in the SM Higgs direction (see Fig. 3), and the resulting effective decay rate is much larger than the inflaton decay rate.

(ii) Analyzing the field dynamics after inflation near the minima of the two-field system, we provided an approximate formula for the reheating temperature, given by Eq. (28), which is entirely different from the standard inflaton decay rate. We emphasize the fact that the approximate formula presented in this paper can be used for generic inflation models that involve two fields in the oscillation epoch after inflation and a naive estimate of the reheating temperature from the inflaton decay is extremely low. Using this two-field analysis as the reheating mechanism, the actual reheat temperature (in the standard inflaton decay case) is found to be much higher than the one naively estimated by the original inflaton decay width. For our inflationary benchmark point, the reheating temperature is estimated to be $T_{rh} \sim 70$ GeV, even in the case of the negligible decay rate of the inflaton itself.

(iii) We investigated the Z_{BL} portal DM in a minimal $\mathrm{U}(1)_{B-L}$ extension of the SM, where the $B-L$ gauge coupling is determined by the requirement from the inflationary observables. For our benchmark parameter choice, the observed DM relic density is reproduced.

(iv) We considered the search for the Z_{BL} gauge boson in current and future lifetime frontier experiments and speculated that the parameter space that satisfies inflationary, reheating, and dark matter constraints simultaneously can be explored in the future. In Fig. 5, we give one benchmark point of $m_{Z_{BL}} = 200$ MeV and $g_{BL} = 10^{-4}$, which will be within the reach of next-generation collider experiments.

In the future, we will look to build upon our studies and understand other SM extensions as a direction of model building for inflation, reheating, dark matter, and neutrino mass frameworks, especially involving the light dark sector. The analytical formula for the reheating temperature we obtained in our studies can be used in several light inflaton models that offer several interesting and particularly complementary experimental probes in the context of cosmological, astrophysical, and laboratory-based searches for new physics beyond the SM.

ACKNOWLEDGMENTS

This work is supported in part by the U.S. Department of Energy Award No. DE-SC0012447 (N. O.).

[1] A. D. Linde, Adv. Ser. Astrophys. Cosmol. **3**, 149 (1987).
[2] A. H. Guth, Adv. Ser. Astrophys. Cosmol. **3**, 139 (1987).
[3] Y. Akrami *et al.* (Planck Collaboration), Astron. Astrophys. **641**, A10 (2020).
[4] F. L. Bezrukov and M. Shaposhnikov, Phys. Lett. B **659**, 703 (2008).
[5] M. Libanov, V. Rubakov, and P. Tinyakov, Phys. Lett. B **442**, 63 (1998).
[6] R. Fakir and W. Unruh, Phys. Rev. D **41**, 1783 (1990).
[7] T. Futamase and K.-i. Maeda, Phys. Rev. D **39**, 399 (1989).
[8] I. Masina, Phys. Rev. D **98**, 043536 (2018).
[9] N. Okada, M. U. Rehman, and Q. Shafi, Phys. Rev. D **82**, 043502 (2010).
[10] R. Kallosh, A. D. Linde, D. A. Linde, and L. Susskind, Phys. Rev. D **52**, 912 (1995).
[11] T. Inagaki, R. Nakanishi, and S. D. Odintsov, Astrophys. Space Sci. **354**, 627 (2014).
[12] A. Ghoshal, D. Mukherjee, and M. Rinaldi, arXiv: 2205.06475.
[13] G. Ballesteros and C. Tamarit, J. High Energy Phys. 02 (2016) 153.
[14] V. N. Senoguz and Q. Shafi, Phys. Lett. B **668**, 6 (2008).
[15] K. Enqvist and M. Karciauskas, J. Cosmol. Astropart. Phys. 02 (2014) 034.
[16] N. Okada, S. Okada, and D. Raut, Phys. Rev. D **95**, 055030 (2017).
[17] S.-M. Choi and H. M. Lee, Eur. Phys. J. C **76**, 303 (2016).

[18] R. Allahverdi, K. Enqvist, J. Garcia-Bellido, and A. Mazumdar, Phys. Rev. Lett. **97**, 191304 (2006).
[19] R. Allahverdi, K. Enqvist, J. Garcia-Bellido, A. Jokinen, and A. Mazumdar, J. Cosmol. Astropart. Phys. 06 (2007) 019.
[20] J. C. Bueno Sanchez, K. Dimopoulos, and D. H. Lyth, J. Cosmol. Astropart. Phys. 01 (2007) 015.
[21] D. Baumann, A. Dymarsky, I. R. Klebanov, L. McAllister, and P. J. Steinhardt, Phys. Rev. Lett. **99**, 141601 (2007).
[22] D. Baumann, A. Dymarsky, I. R. Klebanov, and L. McAllister, J. Cosmol. Astropart. Phys. 01 (2008) 024.
[23] M. Badziak and M. Olechowski, J. Cosmol. Astropart. Phys. 02 (2009) 010.
[24] K. Enqvist, A. Mazumdar, and P. Stephens, J. Cosmol. Astropart. Phys. 06 (2010) 020.
[25] R. Cerezo and J. G. Rosa, J. High Energy Phys. 01 (2013) 024.
[26] S. Choudhury, A. Mazumdar, and S. Pal, J. Cosmol. Astropart. Phys. 07 (2013) 041.
[27] S. Choudhury and A. Mazumdar, arXiv:1403.5549.
[28] N. Okada and D. Raut, Phys. Rev. D **95**, 035035 (2017).
[29] E. D. Stewart, Phys. Lett. B **391**, 34 (1997).
[30] E. D. Stewart, Phys. Rev. D **56**, 2019 (1997).
[31] M. Drees and Y. Xu, J. Cosmol. Astropart. Phys. 09 (2021) 012.
[32] A. Ghoshal, G. Lambiase, S. Pal, A. Paul, and S. Porey, J. High Energy Phys. 09 (2022) 231.
[33] S. Biondini and K. Sravan Kumar, J. High Energy Phys. 07 (2020) 039.
[34] K. Sravan Kumar and P. Vargas Moniz, Eur. Phys. J. C **79**, 945 (2019).
[35] N. Okada, D. Raut, and Q. Shafi, Phys. Lett. B **812**, 136001 (2021).
[36] A. Ghoshal, N. Okada, and A. Paul, Phys. Rev. D **106**, 055024 (2022).
[37] N. Okada and D. Raut, Phys. Rev. D **103**, 055022 (2021).
[38] D. Curtin *et al.*, Rep. Prog. Phys. **82**, 116201 (2019).
[39] A. G. Hessler, A. Ibarra, E. Molinaro, and S. Vogl, J. High Energy Phys. 01 (2017) 100.
[40] G. Bélanger *et al.*, J. High Energy Phys. 02 (2019) 186.
[41] T. Hambye, M. H. G. Tytgat, J. Vandecasteele, and L. Vanderheyden, Phys. Rev. D **98**, 075017 (2018).
[42] S. Heeba and F. Kahlhoefer, Phys. Rev. D **101**, 035043 (2020).
[43] R. N. Mohapatra and N. Okada, Phys. Rev. D **102**, 035028 (2020).
[44] R. N. Mohapatra and N. Okada, Phys. Rev. D **101**, 115022 (2020).
[45] B. Barman and A. Ghoshal, J. Cosmol. Astropart. Phys. 03 (2022) 003.
[46] B. Barman, P. Ghosh, A. Ghoshal, and L. Mukherjee, J. Cosmol. Astropart. Phys. 08 (2022) 049.
[47] A. Das, P. S. B. Dev, and N. Okada, Phys. Lett. B **799**, 135052 (2019).
[48] C.-W. Chiang, G. Cottin, A. Das, and S. Mandal, J. High Energy Phys. 12 (2019) 070.
[49] A. Das, N. Okada, S. Okada, and D. Raut, Phys. Lett. B **797**, 134849 (2019).
[50] A. Ghoshal, L. Heurtier, and A. Paul, arXiv:2208.01670.
[51] B. Barman, P. S. B. Dev, and A. Ghoshal, arXiv:2210.07739.
[52] B. Barman and A. Ghoshal, arXiv:2203.13269.
[53] G. Elor, R. McGehee, and A. Pierce, arXiv:2112.03920.
[54] R. N. Mohapatra and R. Marshak, Phys. Rev. Lett. **44**, 1316 (1980); **44**, 1643(E) (1980).
[55] R. Marshak and R. N. Mohapatra, Phys. Lett. **91B**, 222 (1980).
[56] C. Wetterich, Nucl. Phys. **B187**, 343 (1981).
[57] A. Masiero, J. Nieves, and T. Yanagida, Phys. Lett. **116B**, 11 (1982).
[58] R. N. Mohapatra and G. Senjanovic, Phys. Rev. D **27**, 254 (1983).
[59] A. Davidson, Phys. Rev. D **20**, 776 (1979).
[60] M. Tristram *et al.*, Phys. Rev. D **105**, 083524 (2022).
[61] P. Ade *et al.* (Simons Observatory Collaboration), J. Cosmol. Astropart. Phys. 02 (2019) 056.
[62] S. Aiola *et al.* (ACT Collaboration), J. Cosmol. Astropart. Phys. 12 (2020) 047.
[63] P. Ilten, Y. Soreq, M. Williams, and W. Xue, J. High Energy Phys. 06 (2018) 004.
[64] F. Deppisch, S. Kulkarni, and W. Liu, Phys. Rev. D **100**, 035005 (2019).
[65] A. Ariga *et al.* (FASER Collaboration), Phys. Rev. D **99**, 095011 (2019).
[66] S. Alekhin *et al.*, Rep. Prog. Phys. **79**, 124201 (2016).
[67] M. J. Dolan, T. Ferber, C. Hearty, F. Kahlhoefer, and K. Schmidt-Hoberg, J. High Energy Phys. 12 (2017) 094.
[68] P. Ilten, J. Thaler, M. Williams, and W. Xue, Phys. Rev. D **92**, 115017 (2015).
[69] P. Ilten, Y. Soreq, J. Thaler, M. Williams, and W. Xue, Phys. Rev. Lett. **116**, 251803 (2016).